RSC Advances

ROYAL SOCIETY OF CHEMISTRY

www.rsc.org/advances

A reversible fluorescent-colorimetric chemosensor based on a novel Schiff base for visual detection of CO_3^{2-} in aqueous solution

Anupam Ghorai, Jahangir Mondal, Rukmani Chandra and Goutam K Patra*

Department of Chemistry, Guru Ghasidas Vishwavidyalaya, Bilaspur (C.G)

Abstract

A reversible fluorescent colorimetric chemosensor for rapid detection of carbonate ion has been developed based on a novel *bis*-Schiff base. The chemosensor **L** employed here is easy to synthesize, eco-friendly and cost effective. It exhibits an excellent selectivity and sensitivity towards carbonate ion by change in both absorption and fluorescence intensity. The anion recognition occurs indirectly through coordination of counter metal ion to the Schiff base ligand exhibiting colour change from colourless to yellow. Microstructural features of **L** and **L**+M^+ have been investigated by SEM image. The sensitivity of the absorbance based assay (96 nM) for carbonate ion is the lowest ever reported in the literature. The chemosensor **L** providing rapid response time with sufficiently low detection limit may be useful as a valuable practical sensor for environmental analyses of carbonate ion.

*Corresponding Author: Tel.: 91 7587312992, *E-mail*: patra29in@yahoo.co.in

Introduction

In recent years, the design and synthesis of new sensitive and selective chemosensors that can selectively recognize and signal the presence of anionic species through the naked eye and optical responses has received significant attention because of their potential applications in the environmental, biological and clinical areas.[1] Among various anions commonly present in our environment, the detection and quantification of carbonate is of great importance due to its abundance and ubiquity in natural waters and soil environments mainly as metal carbonates.[2] The major sources of carbonates are the hydrolysis of carbon dioxide into carbonic acid and consequential transformation into carbonates and bicarbonates which involved in rock weathering, mineral precipitation, ocean acidification and climate change.[3] Calcium carbonate being an important material for marine and geological processes is often created as a result of bio-mineralisation and is used by nature to perform many diverse functions in marine organisms including skeleton and shell growth. Carbonate compounds are extensively used in the manufacture of glass, rayon, rubber, plastic, paper, printing ink, cosmetics, toothpaste and food. It is also used as an important candidate for electric vehicle and hybrid electric vehicle power sources where vinylene carbonate is used as additive electrolytes for rechargeable Li-ion batteries.[4] Furthermore, carbonate has vital roles in agricultural planting, soil science,[5] hydrology[6] and geology. [7] In spite of these wide applications in various processes, carbonate ion is toxic in large doses. The strong caustic effect of carbonate to the gastro-intestinal tract may cause severe abdominal pain, vomiting, diarrhoea, collapse and even death.[8] So it is of urgent need to develop a simple, cost effective chemosensor for carbonate having potential of real sample investigation without interference from endogenous substrates.[9] A number of analytical methods have been developed for carbonate ion detection including continuous-flow method,[5] electrochemical method,[10] acoustic method,[11] Fourier transform infrared spectroscopy, [12] gas chromatography,[13] pH-ion-sensitive field-effect transistor,[14] ion selective electrodes[15] and chromo ionophore based optodes[16] etc. However, these methods are cumbersome, time consuming and naked-eye-invisible in most cases. Although many sensors have been reported for the recognition of various anions including phosphate, acetate, sulphide, fluoride and cyanide[17] very few sensors have been reported for carbonate[18] ion till date. Recently Li et al. reported a carbonate sensor based on crystal polymer films.[19] But to the best of our knowledge, a Schiff base or a simple receptor acting as carbonate sensor with potential of easy and onsite

analysis is rarely reported in literature. This possibly results from the difficulty to design a synthetic receptor for carbonate in aqueous media due to its relatively strong alkaline nature and large hydration free energy.[20]

As a part of our ongoing research work[21] in the design and synthesis of chemosensors for anions, cations and neutral molecules, we have synthesized a novel azino *bis*-Schiff base ligand **L**, a 2:1 condensate of benzildihydrazone and syringaldehyde, for the detection of carbonate ion in aqueous solution. The chemosensor **L** demonstrated the presence of carbonate ion both by change in absorbance and fluorescence intensity accompanied by instantaneous colour change from colourless to yellow.

Experimental

General information

UV/Visible spectra were recorded on a Shimadzu UV 1800 spectrophotometer using a 10 mm path length quartz cuvette. Fluorescence spectra were recorded on a Hitachi spectrophotometer. ^{1}H and ^{13}C NMR spectra were recorded on a Bruker Ultrashield 400 using $CDCl_3$ and NMR titrations were carried out by dissolving **L** and sodium carbonate in DMSO-d_6 and D_2O respectively at room temperature and the chemical shifts are reported in δ values (ppm) relative to TMS. High resolution mass (HRMS) spectra were recorded on a Waters mass spectrometer using mixed solvent HPLC methanol and triple distilled water. All the chemicals and metal salts were purchased from Merck. All the anions are of sodium salts and re-crystallized from water (Millipore) before use. Solutions of the receptor **L** (1×10^{-5} M) and anions (1×10^{-4} M) were prepared in CH_3OH–H_2O (2/1, v/v) and H_2O respectively.

Synthesis and characterisation of L

Benzildihydrazone (1.190 g, 5 mmol) is dissolved in 100 mL of anhydrous methanol. To this solution, 1.82 g (10 mmol) of solid syringaldehyde is added with constant stirring. The resulting bright yellowish solution is refluxed for 12h, maintaining dry condition. Then the reaction mixture is cooled to room temperature. Light yellow crystalline solid (suitable for X-ray analysis) precipitates out. It is filtered off, and dried in air. Yield, 2.35 (72%); mp, 202ºC. ^{1}H NMR (400 MHz, $CDCl_3$, TMS): δ 8.30 (s, -HC=N, 2H), 7.89 (d, 4H), 7.39 (dd, 6H), 6.75 (s, 4H), 3.77 (s, $-OCH_3$, 12H) (Fig S1). ^{13}C NMR (400 MHz, $CDCl_3$, δ ppm, TMS): 165.1, 159.4,

147.10, 137.8, 135.3, 130.6, 128.7, 127.7, 125.9, 105.6 and 56.4 (Fig. S2). FTIR/cm-1 (KBr): 692(w), 729 (w), 756 (w), 1114(vs), 1157(m), 1216(s), 1246(m), 1317(s), 1355(s), 1421(m), 1458(s), 1512 (vs), 1597(vs, -C=N), 2937(w), 3080 (w), 3498 (w) (Fig. S3). ESI MS: 567.50 (LH^+, 100%) (Fig. S4). UV-VIS λmax/nm (ε/dm^3 mol^{-1} cm^{-1})(CH_3OH): 345 (40 970). Anal. Calc. for $C_{32}H_{30}N_4O_6$: C, 67.83; H, 5.34; N, 9.89. Found C, 67.77; H, 5.39; N, 9.85%.

X-ray data collection and structural determination

X-ray single crystal data were collected using MoKα (λ = 0.7107 Å) radiation on a BRUKER APEX II diffractometer equipped with CCD area detector. Data collection, data reduction, structure solution/refinement were carried out using the software package of SMART APEX.[22] The structures were solved by direct methods (SHELXS-97)[23] and standard Fourier techniques, and refined on F2 using full matrix least squares procedures of SHELXL-97 incorporated in WinGX.[24] In most of the cases, non-hydrogen atoms were treated anisotropically. Hydrogen atoms were fixed geometrically at their calculated positions following riding atom model. The crystallographic data are listed in Table 1. Structural information has been deposited at the Cambridge Crystallographic Data Center (CCDC 1410686).

Table 1 Crystallographic data and structure refinement parameters for receptor **L**

Formula	$C_{32}H_{30}N_4O_6$
Formula Weight	566.60
Crystal System	Monoclinic
Space group	P21/c (No. 14)
a [Å]	11.840(5)
b [Å]	10.520(5)
c [Å]	23.100(5)
β [°]	96.951(5)
V [$Å^3$]	2856.1(19)
Z	4
D(calc) [g/cm^3]	1.318
μ(MoKα) [/mm]	0.092
F(000)	1192

Crystal Size [mm]	0.14 x 0.16 x 0.20
Temperature (K)	293
Radiation [Å]	MoKα, 0.71073
Θ Min-Max [°]	2.1; 28.8
Dataset	-15: 15 ; -14: 14 ; -30: 30
Total Data	92134
Uniq. Data	7313
R(int)	0.168
Observed data [I > 2.0 sigma(I)]	3856
N_{ref}	7313
N_{par}	380
R	0.0964
wR_2	0.2885
S	1.09

UV-Vis titrations

L (5.66 mg, 0.01 mmol) was dissolved in the solvent mixture $CH_3OH–H_2O$ (2/1, v/v) (10 mL) and 30 μL of it was diluted to 3 mL with the solvent mixture to make a final concentration of 10 μM. Na_2CO_3(10.6mg, 0.1 mmol) was dissolved in10 mL of triple distilled water and 1.5–90 μL of the carbonate ion solution (10 mM) were transferred to the solution of **L** (10 μM) prepared above. After mixing them for a few seconds, UV-Vis spectra were obtained at room temperature.

Fluorescence Titration

L (5.66 mg, 0.01 mmol) was dissolved in 10 mL of mixed solvent $CH_3OH–H_2O$ (2/1, v/v) to make a solution of 1×10^{-3} M and 30 μL of this solution were diluted with 2.97 mL of solvent mixture to make the final concentration of 10 μM. Na_2CO_3 (10.6mg, 0.1 mmol) was dissolved in triple distilled water (10 mL) and 1.5 – 60 μL of this CO_3^{2-} solution (10 mM) were transferred to each receptor solution (10 μM) to give 0.5–20 equiv. After mixing them for a few seconds, fluorescence spectra were obtained at room temperature.

Competition with other anions

For CO_3^{2-}, **L** (5.66 mg, 0.01 mmol) was dissolved in afore-mentioned solvent mixture (10 mL) and 30 μL of it was diluted to 3 mL with the solvent mixture to make a final concentration of 10 μM. Sodium salts of F−, Cl−, Br−, I−, N3−, H_2PO4−, NO3−, OAc−, HCO3− , HSO3− ,CO32- ,SO42-,SO32-,CN-, S2-(0.1 mmol) were dissolved in 10 mL of triple distilled water and 6 μL of each solution (10 mM) were added to 3 mL of the solution of receptor L (10 μM) to give 2 equiv. of anion conc. Then, 6 μL of CO32- solution (10 mM) were added to the mixed solution of each anion and L to make 2 equiv. After mixing them for a few seconds, absorbance spectra were obtained at room temperature.

Job plot measurements

L (5.66 mg, 0.01 mmol) was dissolved in methanol (10 mL). 100, 90, 80, 70, 60, 50, 40, 30, 20, 10 and 0 μL of the **L** solution were taken and transferred to vials. Each vial was diluted with 2.9 mL of a mixed solvent. Na_2CO_3 (0.01 mmol) was dissolved in triple distilled water (10 mL). 0, 10, 20, 30, 40, 50, 60, 70, 80, 90 and 100 μL of the carbonate solution were added to each diluted **L** solution. Each vial had a total volume of 3 mL. After shaking them for a minute, UV-Vis spectra were obtained at room temperature.

Computational details

The GAUSSIAN-09 Revision C.01 program package was used for all calculations.[25] The gas phase geometries of the compound was fully optimized without any symmetry restrictions in singlet ground state with the gradient-corrected DFT level coupled with the hybrid exchange correlation functional that uses Coulomb-attenuating method B3LYP.[26] Basis set 6-31++G was found to be suitable for the whole molecule.

Result and discussion

Synthesis and structure of L

Receptor **L** was obtained by the condensation reaction of benzil dihydrazone and syringaldehyde in methanol with 72% yield (Scheme 1) and characterized by ^{1}H NMR, ^{13}C NMR, IR, ESI-mass spectrometry, elemental analysis and X-ray crystallography. The IR spectra of azino *bis*-Schiff

base **L** showed a broad band at 3498 cm^{-1} for OH stretching vibration. In addition, the band appeared at 1597 cm^{-1} is due to $\gamma_{(C=N)}$ stretching frequency.

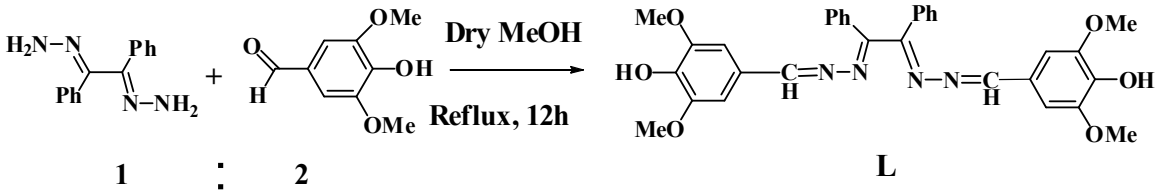

Scheme 1 Synthetic procedure of the receptor **L**

DFT calculations were performed on the molecule **L**. The geometry optimizations staring from Gauss-view structure of **L** lead to a global minimum as stationary level. The optimized structure of the **L** has been shown in Fig. 1. A schematic representation of the energy of MOs and contours of selected HOMO and LUMO orbitals of **L** are presented in Fig. 2. The HOMO to LUMO energy gap for **L** is 7.40683 eV.

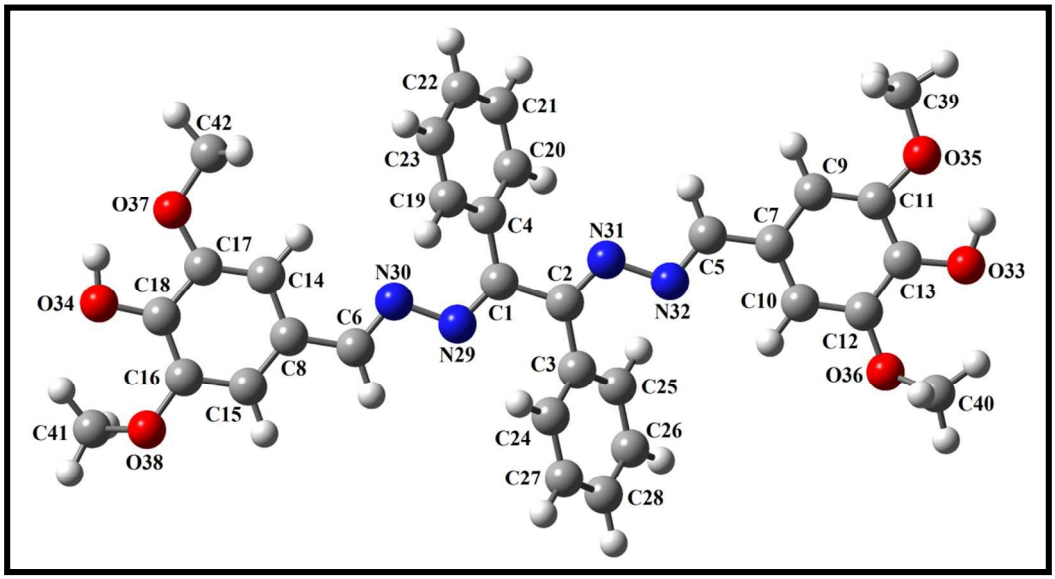

Fig. 1 Geometry optimized diagram of the molecule **L.**

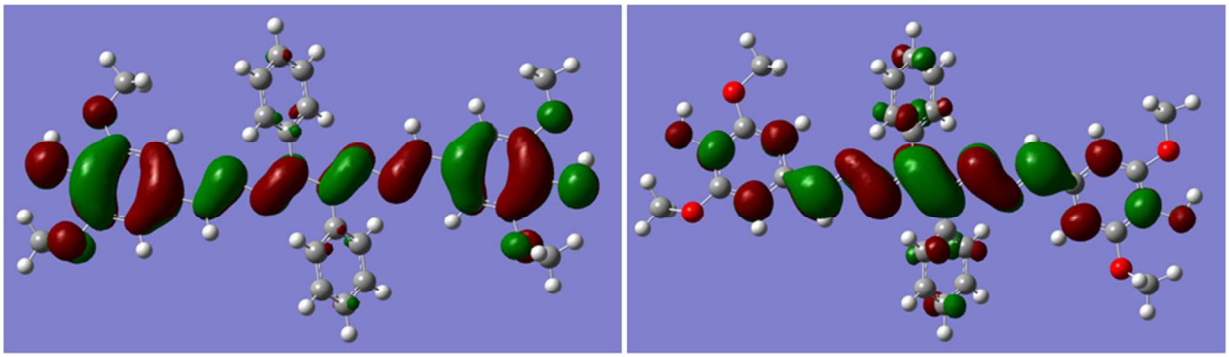

Fig. 2 The contour diagrams of HOMO and LUMO of **L.**

Crystals of **L** were obtained by slow evaporation of methanolic solution. Single crystal-XRD analysis of **L** reveals that the molecule crystallizes in $P2_1/c$ space group and the 'z' value is 4. The ORTEP diagram of **L** is shown in Fig. 3. The molecular structure is based on the $-C^1$-N^1-N^2-C^8-C^9-N^3-N^4-C^{10}- backbone where two unsubstituted phenyl rings are attached to the middle C-atoms (C^8 and C^9) and two substituted phenyl rings are attached to terminal C-atoms (C^1 and C^{10}).

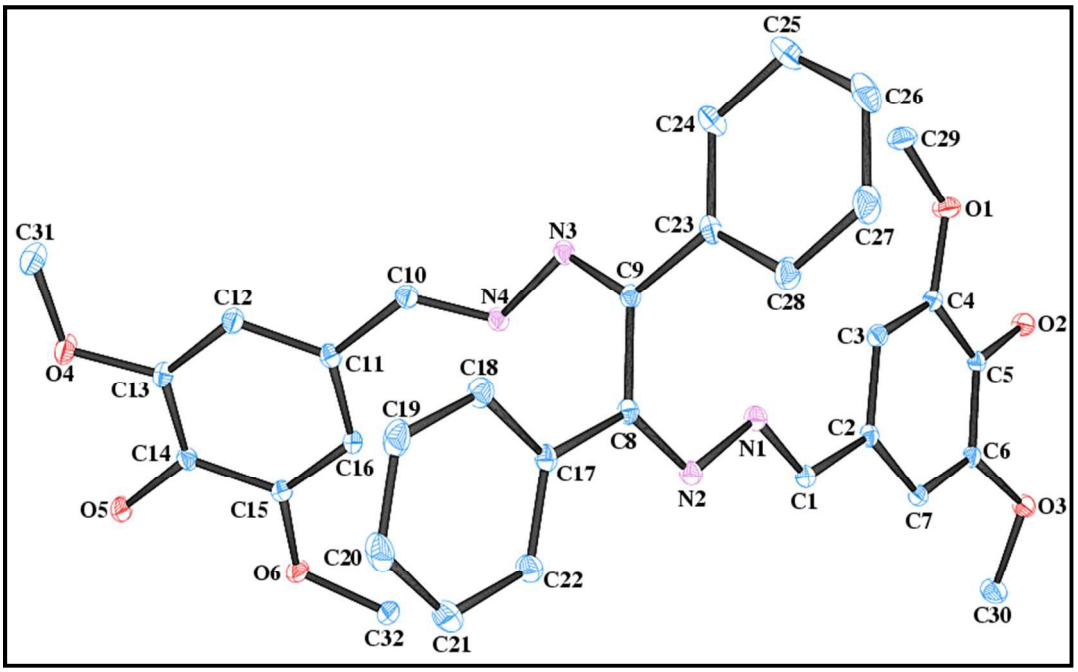

Fig. 3 ORTEP diagram of the **L** molecule (H atoms are omitted for clarity).

Absorption studies of L towards different anions

The colorimetric selective sensing abilities of chemosensor **L** were primarily investigated by UV-Vis absorption spectrometry in a $CH_3OH–H_2O$ solution (2:1, v/v) with various metal cations (Al^{3+}, Mg^{2+}, Mn^{2+}, Fe^{3+}, Ba^{2+},Co^{2+}, K^{+}, Ni^{2+}, Ca^{2+}, Cu^{2+}, Cr^{3+}, Zn^{2+}, Cd^{2+}, Na^{+}, Hg^{2+} and Ag^{+}) (Fig. S5) and anions (SO_4^{2-}, SO_3^{2-}, HSO_3^{-}, F^{-}, OAc^{-}, Cl^{-}, Br^{-}, I^{-}, $H_2PO_4^{-}$, HCO_3^{-}, N_3^{-}, NO_3^{-}, CO_3^{2-}) (Fig. 4). Only the addition of carbonate induced distinct spectral changes while other anions did not induce any spectral change. We further checked the absorption behaviour of **L** with the anions S^{2-} and CN^{-}. Both CN^{-} and S^{2-} exhibit almost no change in the absorption spectra as well as in visible colour. But in much higher concentration, S^{2-} (8×10^{-3} M) induces a decrease in absorption intensity at 345 nm with hardly perceptible colour change of **L** (Fig. S6).

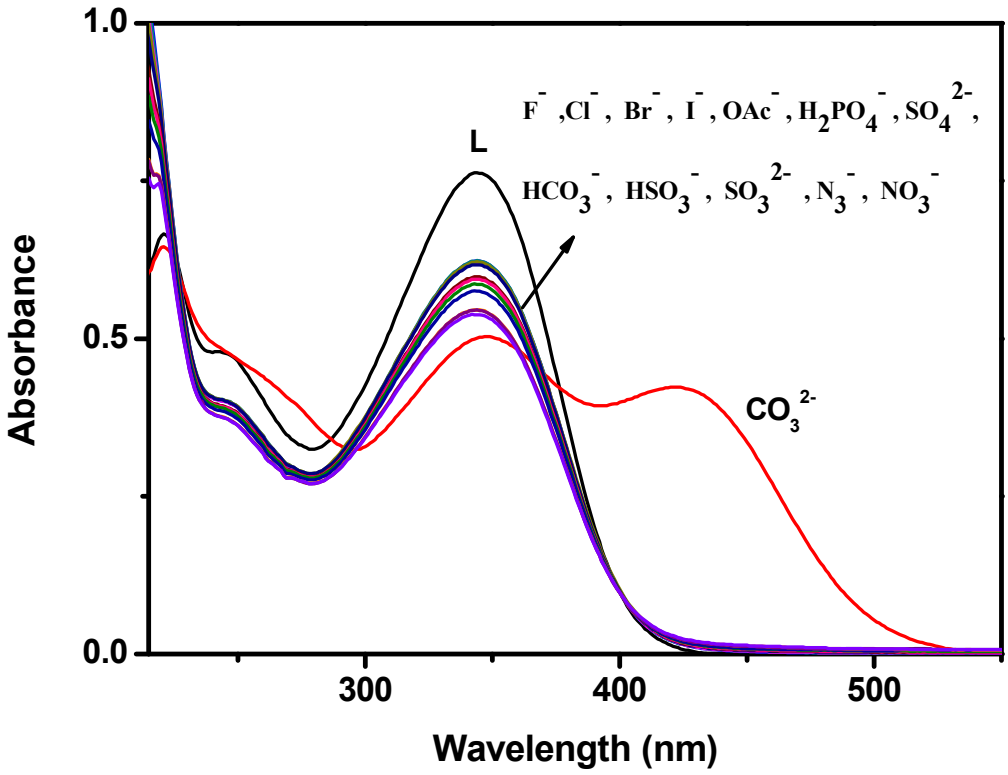

Fig. 4 Changes in the absorption spectra of **L** (10 μM) in the presence of 2 equiv. of different anions.

The probe **L** without carbonate exhibited a strong UV-vis absorption band at 345 nm which was attributed to the photo-induced electron transfer (PET) transition in the molecule. Addition of carbonate to a solution of **L** led to an obvious absorption enhancement at 423 nm

with concomitant decrease in absorption intensity at 345 nm. Consistent with this change in the UV-Vis spectra, the solution of **L** resulted in an immediate colour change from colourless to yellow with the carbonate ion (Fig. S7), indicating that receptor **L** can serve as a 'naked-eye' carbonate indicator in aqueous solution.

The selectivity behaviour over a wide range of back ground anions is obviously a matter of importance for an excellent sensing material. The exclusive selectivity of chemosensor **L** towards carbonate ion was further studied ratiometrically.

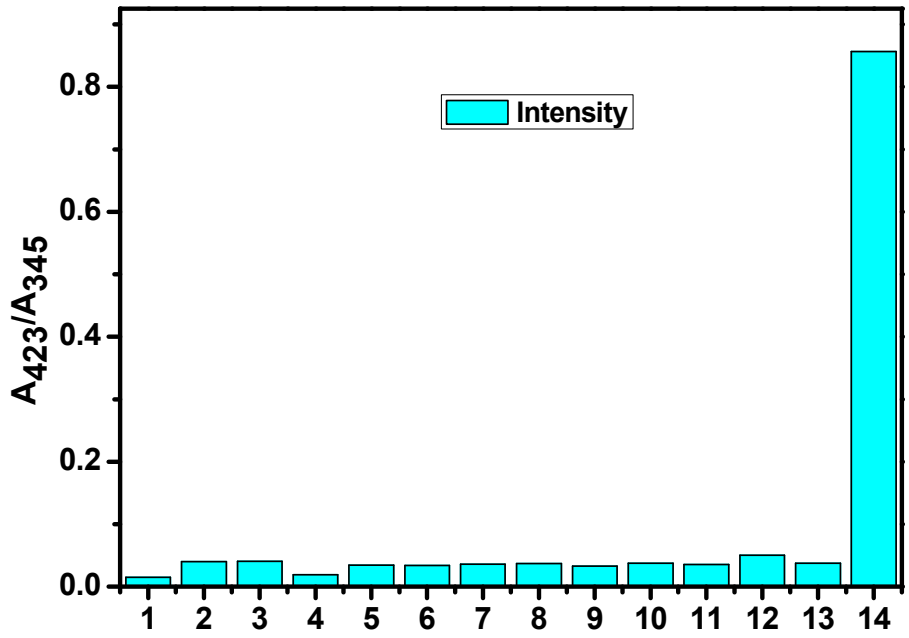

Fig. 5 The bar graph showing the relative absorption intensity of **L** upon treatment with various anions (1.SO_4^{2-}; 2.SO_3^{2-}; 3. HSO_3^-; 4.F^-; 5.OAc^-; 6.Cl^-; 7.Br^-; 8.I^-; 9.$H_2PO_4^-$; 10.HCO_3^-; 11.N_3^-; 12.NO_3^-; 13.**L** and 14.CO_3^{2-}).

However, the absorption study carried out with common metal cations and other anions showed no significant change, indicating their noninteractive nature with **L**. In Fig. 5, a bar graph showing the relative absorption intensity of **L** upon treatment with various anions has been given. To further check the practical applicability of receptor **L** as a carbonate ion selective chromogenic receptor, a competitive experiment was carried out with 2 equiv. of CO_3^{2-} in the presence of 2 equiv. of other anions in an aqueous solution (Fig. 6). It was found that any other

anions under experiment did not interfere with the detection of CO_3^{2-} by **L**. This indicates that under signalling conditions, the possible interference by them is not a practical problem in carbonate sensing by **L**.

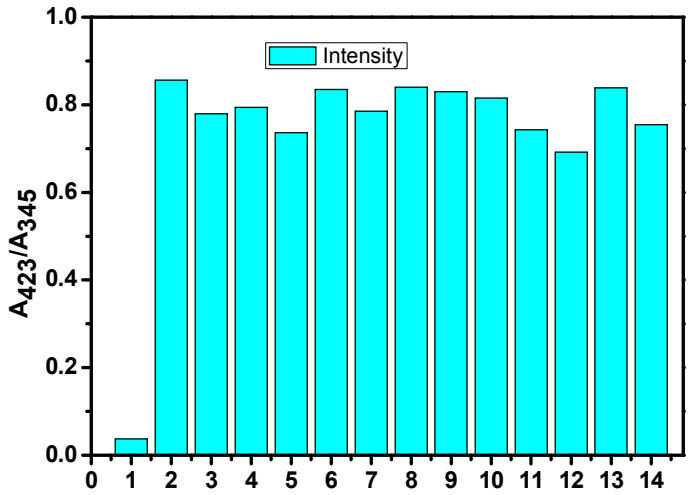

Fig. 6 Competitive experiment in presence of other anions (1. **L**; 2. **L**+CO_3^{2-}; 3. **L**+CO_3^{2-}+SO_3^{2-}; 4. **L**+CO_3^{2-}+HSO_3^-; 5. **L**+CO_3^{2-}+F^-; 6. **L**+CO_3^{2-}+OAc^-; 7. **L**+CO_3^{2-}+Cl^-; 8. **L**+CO_3^{2-}+Br^-; 9. **L**+CO_3^{2-}+I^-; 10. **L**+CO_3^{2-}+$H_2PO_4^-$; 11. **L**+CO_3^{2-}+HCO_3^-; 12. **L**+CO_3^{2-}+N_3^-; 13. **L**+CO_3^{2-}+NO_3^-; and 14. **L**+CO_3^{2-}+SO_4^{2-}).

The recognition ability of probe **L** towards carbonate ion was established upon titration of the probe solution with variable concentrations of carbonate ion followed by subsequent measurement of absorption spectra (Fig. 7).

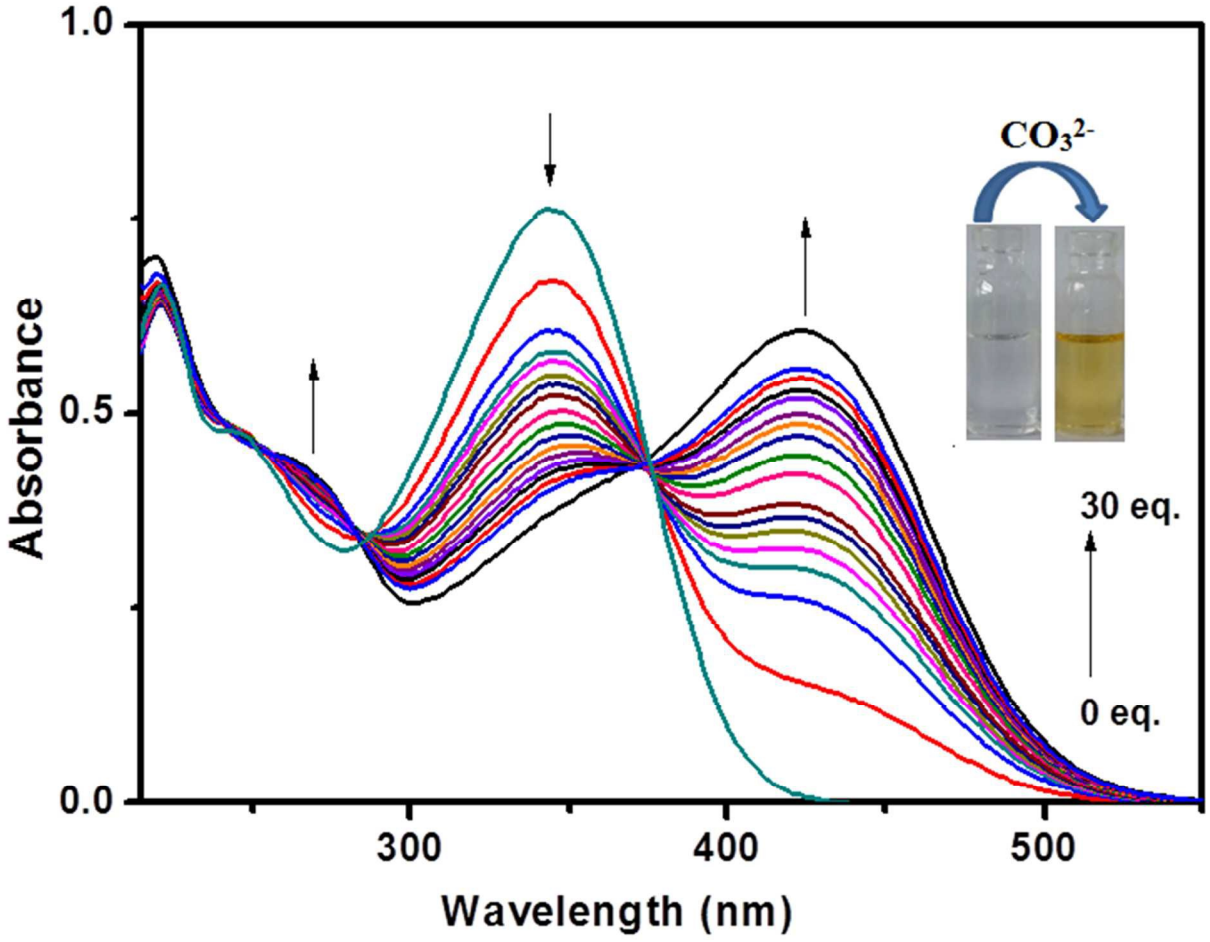

Fig. 7 Change in the absorption spectra of **L** after the addition of CO_3^{2-} upto 30 equiv.

Interestingly, probe **L** exhibits two well-defined isosbestic points at 285 and 375 nm in the absorption spectra upon increasing concentration of carbonate. The isosbestic point at 375 nm indicates equilibrium between two species, the free ligand and metal bonded ligand. In the UV–visible titration experiment, the blue-shifted band around 345 nm went-down while the intensity of the newly red shifted band at 423 nm triggered by carbonate ion continuously increases with successive increment of carbonate ion (0–30 equiv.) into the probe solution as shown in Fig. 7. We propose that the blue-shifted band, which is initially present, corresponds to the free receptor **L** and the red-shifted band corresponds to the metal ion-bonded species. The prominent bathochromic shift of about 78 nm occurred on addition of carbonate led us to propose that the π conjugate system of **L** underwent intramolecular charge transfer (ICT) from donor to the acceptor upon excitation by light through de-protonation of probe **L** by carbonate ion. Here Na_2CO_3 gets hydrolysed to produce NaOH which causes this de-protonation followed

by subsequent metallation. Binding of Na^+ ion with **L** affected the efficiency of ICT leading to decrease in intensity at 345 nm. To identify the ICT property of **L**, we have checked the change of its absorption spectra in several solvents such as dimethyl sulfoxide, methanol, ethanol and acetonitrile because it has been reported that the solvent dipole can relax the ICT excited by polar solvents.[27] As shown in Fig. S8 and summarized in Table 2, the absorption spectra of **L** featured a marginal red-shift of the absorption maxima ($\Delta\lambda_{abs}$ = 9 nm), indicating an apparent solvent dependence of the absorption band. In order to confirm whether the colour change and corresponding absorbance change occurs due to ICT through de-protonation mechanism the interaction between the probe **L** and OH^- was carried out. UV-Vis spectral change of **L** on addition of OH^- was almost similar as observed in case of carbonate ion demonstrating the de-protonation mechanism (Fig S9).

Table 2 Absorption properties of **L** in various solvents

Solvent	**λ_{abs}[nm](logε)**
MeOH	345 (7.23)
Acetonitrile	352 (7.14)
Chloroform	347 (7.21)
DMSO	354 (7.11)

Therefore, this solvatochromic behaviour demonstrates the occurrence of the ICT transition in receptor **L**. Fig. S10 which highlights the ratiometric response of the probe **L** on addition carbonate in narrow range shows that the A_{423}/A_{345} curve becomes a plateau at [CO_3^{2-}]/[**L**] ratio over 1. The Job plot analysis also indicated a 1:1 stoichiometric adduct of receptor **L** and Na^+ ion (Fig. S11). The fact that the sensing of CO_3^{2-} by chemosensor **L** does not depend on counter metal ion, can be established by the similar type of absorbance spectra shown by **L** with potassium carbonate (Fig. S12). To our pleasure, the detection limit calculated from the titration profile was found to be 96 nM (Fig. S13), which, to the best of our knowledge, is the lowest ever reported in the literature.

Fluorescence studies

The fluorescence behaviours of chemosensor **L** is also prominent in distinguishing CO_3^{2-} from other anions (SO_4^{2-}, SO_3^{2-}, HSO_3^-, F^-, OAc^-, Cl^-, Br^-, I^-, $H_2PO_4^-$, HCO_3^-, N_3^-, NO_3^-) (Fig. 8). Upon excitation at 340 nm at room temperature **L** exhibits little emission with a low

fluorescence quantum yield (Φ = 0.0157) along with other anions except for CO_3^{2-} (Φ = 0.427). The low fluorescence intensity of **L** can be ascribed to the photo-induced electron transfer (PET) process. On addition of CO_3^{2-}, **L** gets attached to the metal ion through the terminal hydroxyl groups and thereby hinders the PET process resulting a significant fluorescence enhancement of the **L**–$\mathbf{M}^+$ adduct accompanied by a prominent blue shift of 36 nm. The selectivity experiment is further carried out using HEPES buffer to maintain a constant pH medium of pH = 8.0. It also shows similar result as observed in absence of buffer (Fig. 9).

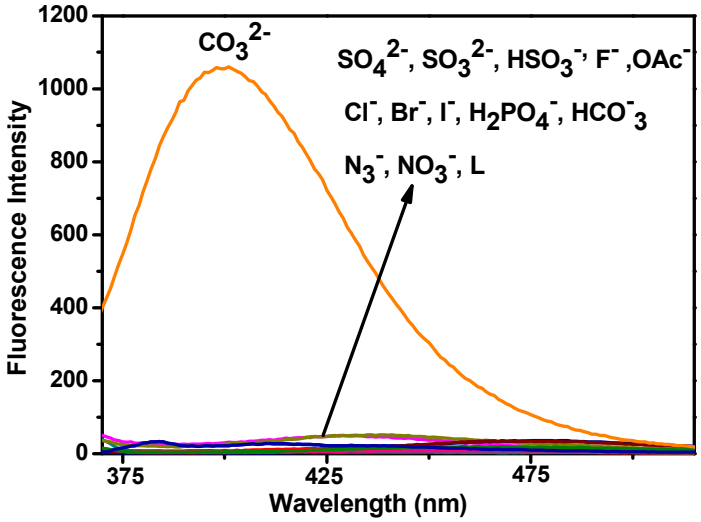

Fig. 8 Fluorescence spectra of **L** (10 μM) before and after addition of various anions (2 equiv.).

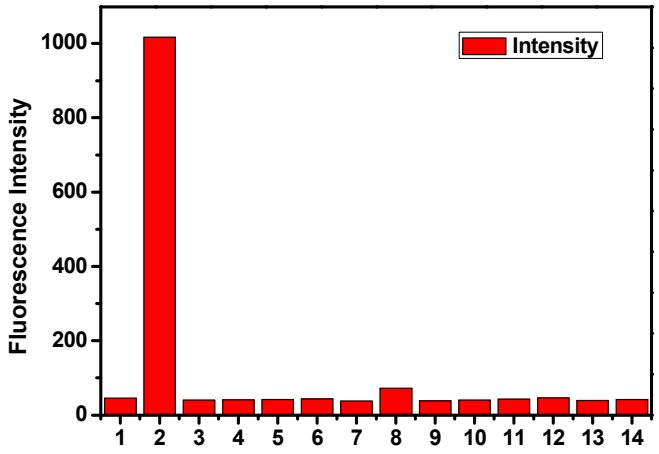

Fig. 9 Relative fluorescence of L in presence of different anions (1. Only **L**; 2. **L**+ CO_3^{2-}; 3. **L**+ F^-; 4. **L** + Cl^-; 5. **L**+ Br^-; 6.**L**+ I^-; 7. **L**+ N_3^-; 8.**L**+ HCO_3^-; 9. **L**+ NO_3^- ; 10. **L**+ SO_4^{2-}; 11. **L** + SO_3^{2-}; 12. **L**+HSO_3^- ; 13. **L** + OAc^- and 14. **L**+ $H_2PO_4^-$ using HEPES buffer.

A quantitative investigation of the binding affinity of **L** with Na^+ on addition of Na_2CO_3 was performed by a fluorescence titration (Fig. 10). It revealed that the emission intensity at 398 nm monotonically increased upon gradual addition of CO_3^{2-} up to 20 equiv. The inset plot of (Fig. 10) elaborates the titration data in narrow range implying that the reaction gets almost completed on addition of one equivalent of CO_3^{2-}.

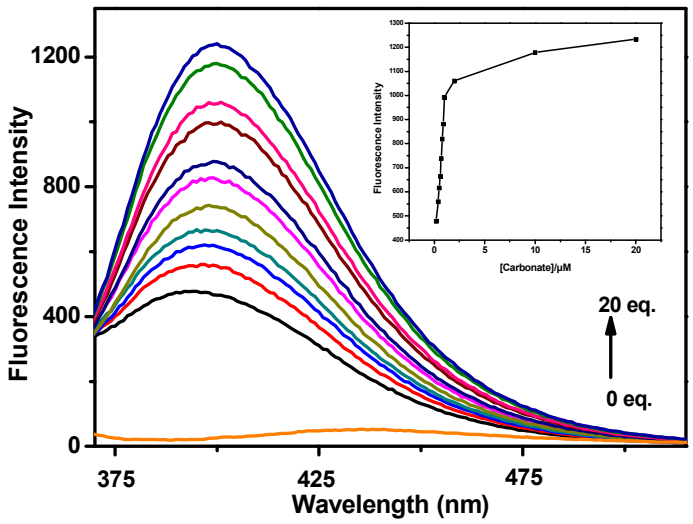

Fig. 10 Fluorescence spectra of **L** (10 μM, λ_{ex} = 340 nm) after addition of increasing amounts of CO_3^{2-} (upto 20 equiv.) in MeOH-H_2O (2:1, v/v) at room temperature. Inset: intensity at 398 nm vs the number of equiv. of CO_3^{2-} added.

Sensing mechanism, ^{1}H NMR and HRMS spectral studies of the probe and the adduct

In order to obtain better insight into the sensing mechanism, ^{1}H NMR and mass spectral studies of carbonate have been carried out. The presence of two terminal hydroxyl groups in Schiff base receptor was observed to play a vital role in sensing mechanism (Scheme 2). The disappearance of –OH band (which was present in IR spectra of free ligand) in IR spectra of metal bonded adduct (Fig. S14) stands in support of involvement of hydroxyl group in sensing mechanism.

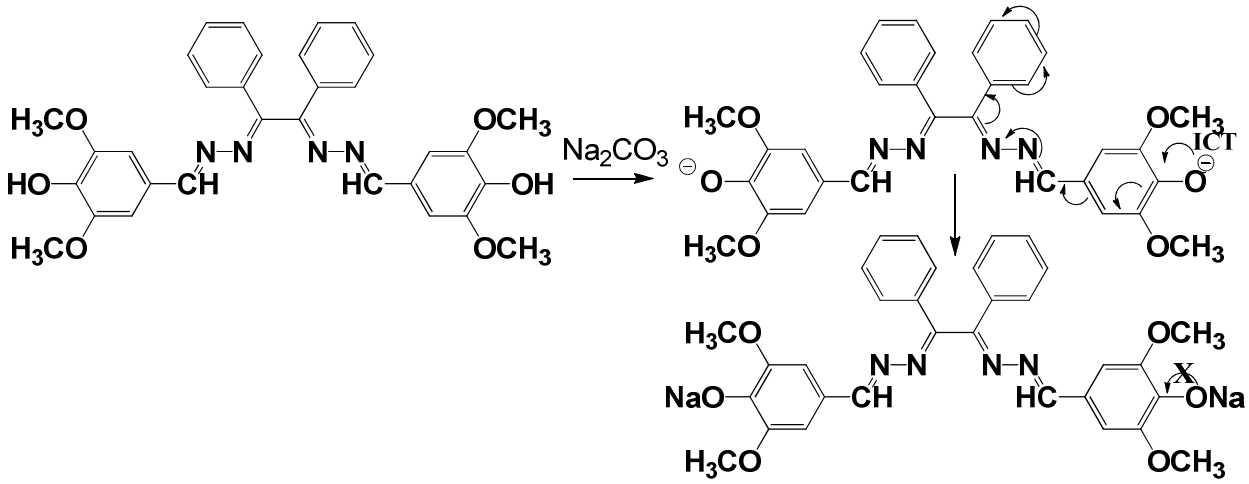

Scheme 2 Proposed sensing mechanism

The mechanism is also well corroborated by ^{1}H NMR spectra (Fig. S15), where the peak at 9.05 ppm for –OH proton in free receptor was completely vanished with slight displacement of other peaks on addition of one equivalent of sodium carbonate due to binding of Na^+ ion to terminal hydroxyl group of receptor. In addition, the formation of a 1 : 2 adduct between **L** and Na^+ was further confirmed by the appearance of a peak at m/z 611, assignable to [**L** + $2Na^+$] in the ESI/MS (Fig. S16). Moreover fluorescence behaviour of the probe **L** before and after the addition of carbonate was examined under different pH conditions (Fig.S17). It was observed that there was no significant change in emission intensity at 398 nm for the probe (10 μM) alone in the pH range 2-9 while after addition of carbonate ions into probe solution, a drastic enhancement in the emission signal centred at 398 nm appeared in the pH span of 5-8. At lower pH range 2-4, the fluorescence intensity of the probe, on addition of carbonate ions, abruptly

falls and similar observation was also observed after pH > 8. But to be a pH sensor it should be pH responsive at different pH conditions. So it can be concluded that the probe is not a pH sensor.

SEM image

To understand the aggregation property of **L** and **L** + **Na_2CO_3** and its effect on their chemo-sensing property, scanning electron microscope (SEM) imaging was carried out. **L** and **L** + **Na_2CO_3** adduct possess charge transfer, π–π stacking, and van der Waals force of attraction which cause the compounds to form agglomerate material and framework like structure respectively (Fig. S18). The framework like structure results due to strong interaction of the Na^+ ion with the ligand **L**.

Reversibility is a prerequisite in developing novel chemosensors for practical application. In detection of carbonate ion reversibility is rarely observed.[28] The reversibility of the recognition process of receptor **L** was performed by adding an Na^+ bonding agent, CH_3COOH (Fig. 11). The addition of CH_3COOH to a mixture of receptor **L** and Na_2CO_3 resulted in appearance of peak at 345 nm with diminution of the absorption intensity at 423 nm, indicating the regeneration of the free receptor **L**. The absorption band at 423 nm was recovered by the addition of Na_2CO_3 again. Such reversibility is important for the fabrication of devices to sense carbonate ion.

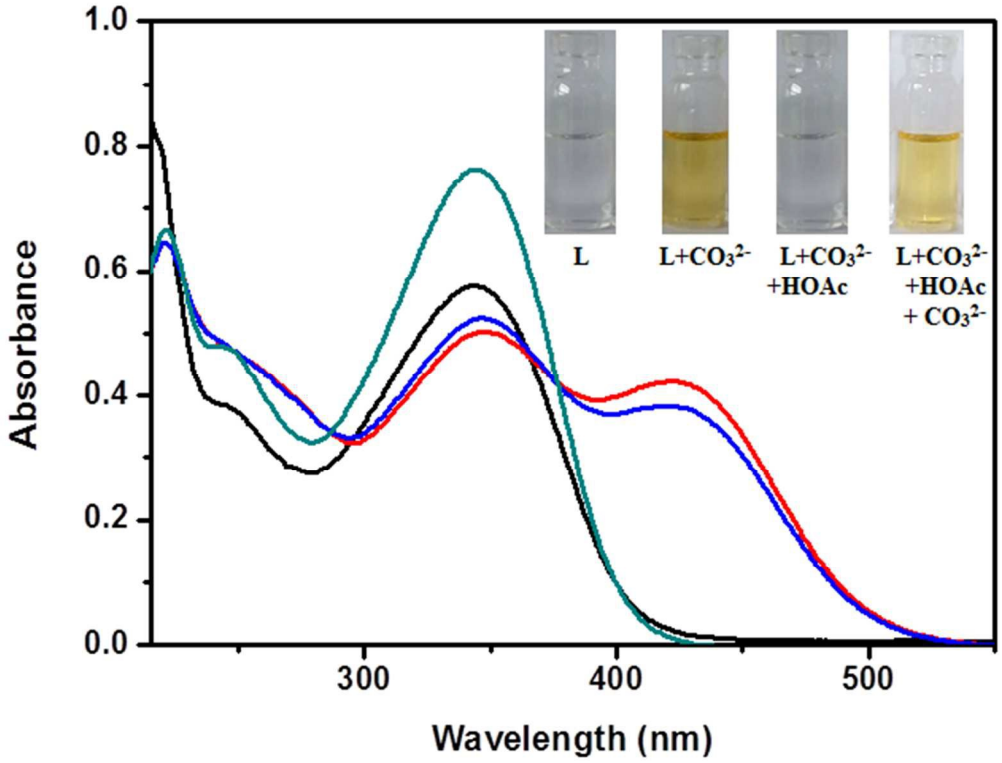

Fig. 11 Reversibilty test of **L** with CH_3COOH (Green trace, **L**; red trace **L**+Na_2CO_3; black trace, **L**+Na_2CO_3 +**HOAc**; blue trace, **L**+Na_2CO_3+**HOAc** + Na_2CO_3).

The quick response time for a sensing material is a prerequisite for practical applicability. To understand the carbonate binding reaction time with probe **L**, the absorption spectra of probe **L** was recorded by variable time interval and the results revealed that the response in ratiometric absorption change started immediately upon carbonate addition and completed within 1 min as shown in the absorption spectra at different time intervals (Fig. S19). It was observed that ratiometric absorbance remained almost constant up to 10 min on addition of 2 equiv. of carbonate ion.

Application of chemosensor L

To check the practical application, the test kits were utilized to sense carbonate among different competing anions. As shown in Fig. 12, when the test kits coated with **L** were added to different anion solutions, the obvious colour change was observed only with carbonate in aqueous solution. Therefore, the test kits coated with the chemosensor **L** solution would be convenient for detecting carbonate. These results showed that chemosensor **L** could be a valuable practical sensor for environmental analyses of carbonate.

Fig. 12 Photographs of the test kits with **L** (0.5 mM) for detecting carbonate ion among other anions.

The applicability of the chemosensor **L** towards real sample analysis was investigated by employing distilled water, tap water and river water under the same conditions (Fig. S20). Almost no fluorescence enhancement was observed in case of distilled water for all concentration of carbonate ion in comparison to the chemosensor **L** alone. But in case of tap water and river water, there occur little enhancement in fluorescence intensity due to presence of carbonate ion in those water samples. However the results obtained suggests that the background ions present in the water samples have little influence in detection of carbonate ion.

Conclusion

In summary we have developed a novel *bis* Schiff base sensor for visual detection of carbonate in aqueous solution. The chemosensor L employed is easy to synthesize, eco-friendly, and cost effective. It exhibits an excellent selectivity and sensitivity towards carbonate by changes in both absorption and fluorescence intensity. The detection limit (96 nM) is the lowest ever reported in the literature. The chemosensor **L** proposed by us has the potentiality in detecting carbonate ions in real samples. On the basis of these results, we believe that the chemosensor **L** may be useful as a valuable practical sensor for environmental analyses of carbonate.

Acknowledgements

G.K.P would like to thank the Department of Science and Technology and Department of Biotechnology, Government of India, New Delhi for financial support and Dr. Rajat Saha for various help.

Reference

1. (a) S. Mizukami, T. Nagano, Y. Urano, A. Odani and K.A. Kikuchi, *J. Am. Chem. Soc.,* 2002, **124**, 3920-3925;(b) R.M. Duke, E.B. Veale, F.M. Pfeffer, P.E. Kruger and T. Gunnlaugsson, *Chem. Soc. Rev.,* 2010, **39**, 3936-3953; (c) J. Shao, H. Lin and H.-K. Lin, *Talanta,* 2008, **75**, 1015-1020; (d) B. Kuswandi, W. Verboom and D. N. Reinhoudt, *Sensors,* 2006, **6**, 978-1017; (e) K. Ghosh and S. Adhikari, *Tetrahedron Lett*., 2006, 47, 8165-8169; (f) A.K. Jain, J. Raisoni, R. Kumar and S. Jain, *Int. J. Environ. Anal. Chem*., 2007, **87**, 553-563; (g) G. A. E. Mostafa, *Int. J. Environ. Anal. Chem*., 2008, **88**, 435-446; (h) M. T. Oms, P. A. C. Jongejan, A. C. Veltkamp, G. P. Wyers and J. Slanina, *Int. J. Environ. Anal. Chem.,* 1996, **62**, 207-218.
2. (a) M. Descostes, C. Beaucaire, F. Mercier, S. Savoye, J. Sow and P. Zuddas, *Bull. Soc. Geol. France*, 2002, **173**, 265-270; (b) C. Su and D.L. Suarez, *Clays Clay Miner,* 1997, **45**, 814-825; (c) L.D. Chen, D. Mandal, G. Pozzi, J.A. Gladysz and P. Buhlmann, *J. Am. Chem. Soc.,* 2011, **133**, 20869-20877.
3. A. H. England, A. M. Duffin, C. P. Schwartz, J. S. Uejio, D. Prendergast and R. J. Saykally, *Chem. Phys. Lett*., 2011, **514**, 187-390.
4. (a) A.C. Tas, *Int. J. Appl. Ceram*. *Technol*, 2009, **6**, 53-64; (b) R. Demichelis, P. Raiteri, J.D. Gale, D. Quigley and D. Gebauer*, Nat. Commun*., 2011,1604-1611; (c) H. Zhao, S. -J. Park, F. Shi, Y. Fu, V. Battaglia, P. N. Ross and G. Liu, *J. Electrochem. Soc.,* 2014, **161**, A194-A197; (d) D. Aurbach, J. S. Gnanaraj, W. Geissler and M. Schmidt, *J. Electrochem. Soc.* 2004, **151**, A23-A30; (e) C. Han, Z. Cui, Z. Zou, D. Sabahaiti, and H. Li, *Photochem. Photobiol. Sci*., 2010, **9**, 1269-1273.
5. M. Zougagh, A. Ríos, M. Valcárcel, *Talanta*, 2005, **65**, 29–35.
6. Y. S. Choi, L. Lvova, J. H. Shin, S. H. Oh, C. S. Lee, B. H. Kim, G. S. Cha, H. Nam, *Anal.Chem.,* 2002, **74**, 2435–2440.
7. R.V. Morris, S.W. Ruff, D.W. Ming, R. E. Arvidson, B. C. Clark, D. C. Golden, K. Siebach, G. Klingelhöfer, C. Schröder, I. Fleischer, A.S. Yen, S.W., *Science*, 2010, **329**, 421–424.
8. A.K. Jain, V.K. Gupta and J.R. Raisoni*, Electrochim. Acta.,* 2006, **52**, 951-957.
9. N. Abramova, S. Levichev and A. Bratov, *Talanta,* 2010, **81**, 1750-1754.
10. H.K. Lee, H. Oh, K.C. Nam, S. Jeon, *Sens. Actuator B*, 2005, **106**, 207–211.

11. O. Dóka, D. Bicanic, M. Szücs, M. Lubbers, *Appl. Spectrosc.,* 1998, **52**, 1526–1529.

12. E. E. Burt and A. H. Rau, *Drug Dev. Industrial Pharm.,* 1994, **20**, 2955–2964.

13. R.G. Amundson, J. Trask and E. Pendall, *Soil Sci. Soc. Am. J.*, 1988, **52**, 880-883.

14. (a) K. Tsukada, Y. Miyahara, Y. Shibata and H. Miyagi, *Sens. Actuator B*, 1990, **2**, 291-295; (b) J. H. Shin, H. J. Lee, C. Y. Kim, B. K. Oh, K. L. Rho, H. Nam and G.S. Cha, *Anal. Chem.,* 1996, **68**, 3166-3172.

15. (a) H. J. Lee, I. J. Yoon, C. L. Yoo, H. -J. Pyun, G. S. Cha and H. Nam, *Anal. Chem*., 2000,**7 2**, 4694-4699; (b) H. K. Lee, H. Oh, K. C. Nam and S. Jeon, *Sens. Actuator B*, 2005, **106**, 207-211; (c) R. K. Meruva and M. E. Meyerhoff, *Biosens. Bioelectron.*, 1998, **13**, 201-212.

16. W.E. Morf, K. Seiler, B. Lehmann, C. Behringer, K. Hartman and W. Simon, *Pure Appl. Chem.*, 1989, **61**,1613-1618.

17.(a) N. Kaura, J. Singha, G. Dhakaa, R. Ranib and V. Luxami, *Supramolecular Chemistry*, 2015, **27**, 453–459; (b) L. J. Tang, M. J. Cai, Z. L. Huang, K. L. Zhong, S. H. Hou, Y. J. Bian, R. Nandhakumar, *Sens. Actuators B*, 2013, **185**, 188–194; (c) L. J. Tang, M. J. Cai, P. Zhou, J. Zhao, K. L. Zhong, S. H. Hou, Y. J. Bian, *RSC Adv.* 2013, **3**, 16802–16809; (d) L. J. Tang, P. Zhou, K. L. Zhong, S. H. Hou, *Sens. Actuators B*, 2013, **182**, 439–445; (e) Z. -B. Zheng, Z. -M. Duan, Y. -Y. Ma and K. -Z. Wang, *Inorg. Chem*., 2013, **52**, 2306–2316; (f) D. Zhang, X. Jiang, H. Yang, Z. Su, E. Gao, A. Martinez, G. Gao, *Chem. Commun.,* 2013, **49**, 6149–6151; (g) S. -I. Kondo, R. Takai, *Org. Lett.,* 2013, **15**, 538–541; (g) V. Reena, S. Suganya, S. Velmathi, *Journal of Fluorine Chemistry,* 2013, **153**, 89–95.

18. (a) G. Hennrich, H. Sonnenschein, U. Resch-Genger, *Tetrahedron Lett.* , 2001, **42**, 2805–2808; (b) H. Cuiping, C. Zhimin, Z. Zhilong, T. Demei and L. Haibing, *Photochem. Photobiol. Sci*., 2010, **9**, 1269 –1273;(c) J. Vaněk, P. Lubal, P. Hermann and P. Anzenbacher. Jr, *J Fluoresc,* 2013, **23**, 57–69.

19. L. Li, B. Zhao,Y. Long, J. -Ming Gao, G. Yang, C. –H. Tungdand and K. Song, *J. Mater. Chem., C*DOI: 10.1039/c5tc02253c.

20. Y. Marcus, *J. Chem. Soc. Faraday Trans.*, 1991, **87**, 2995–2999.

21. (a) A. Ghorai, J. Mondal, R. Chandra and G. K. Patra, *Dalton Trans*., 2015, **44**, 13261;(b) A. Ghorai, J. Mondal, R. Chandra and G. K. Patra, *Analytical Methods*, 2015, DOI:10.1039/C5AY01465D.

22. *SMART & SAINT Software Reference manuals*, *version 5.0; Bruker AXS Inc*.: Madison, WI, 1998.

23. G. M. Sheldrick, *Acta Cryst.*, 2008, **A64**, 112.

24. L. J. Farrugia, *WinGX: An Integrated System of Windows Programs for the Solution, Refinement and Analysis for Single Crystal X-ray Diffraction Data, version 1.80.01*; Department of Chemistry: University of Glasgow, 2003. *J. Appl. Crystallogr.*, 1999**,** 32837.

25. M. J. Frisch, G. W. Trucks, H. B. Schlegel, G. E. Scuseria, M. A. Robb, J. R. Cheeseman, G. Scalmani, V. Barone, B. Mennucci, G. A. Petersson, H. Nakatsuji, M. Caricato, X. Li, H. P. Hratchian, A. F. Izmaylov, J. Bloino, G. Zheng, J. L. Sonnenberg, M. Hada, M. Ehara, K. Toyota, R. Fukuda, J. Hasegawa, M. Ishida, T. Nakajima, Y. Honda, O. Kitao, H. Nakai, T. Vreven, J. A. Montgomery, Jr., J.E. Peralta, F. Ogliaro, M. Bearpark, J. J. Heyd, E. Brothers, K. N. Kudin, V. N. Staroverov, R. Kobayashi, J. Normand, K. Raghavachari, A. Rendell, J. C. Burant, S. S. Iyengar, J. Tomasi, M. Cossi, N. Rega, J. M. Millam, M. Klene, J. E. Knox, J. B. Cross, V. Bakken, C. Adamo, J. Jaramillo, R. Gomperts, R. E. Stratmann, O. Yazyev, A. J. Austin, R. Cammi, C. Pomelli, J.W. Ochterski, R. L. Martin, K. Morokuma, V.G. Zakrzewski, G.A. Voth, P. Salvador, J. J. Dannenberg, S. Dapprich, A. D. Daniels, Ö. Farkas, J. B. Foresman, J.V. Ortiz, J. Cioslowski, and D. J. Fox. *Gaussian 09, Revision C.01, Gaussian Inc*., Wallingford, CT, 2009.

26. (a) A.D. Becke, *J. Chem. Phys*., 1993, **98**, 5648; (b) C. Lee, W. Yang and R.G. Parr., *Phys. Rev. Sect. B*, 1988, **37**, 785.

27. (a) K. C. Song, H. Kim, K. M. Lee, Y. S. Lee, Y. Do and M. H. Lee, *Sens. Actuators, B,* 2013, **176**, 850–857;(b) S. Maruyama, K. Kikuchi, T. Hirano, Y. Urano, T. Nagano and A. Novel, *J. Am. Chem. Soc.*, 2002, **124**, 10650–10651.(c) A. P. Silva, H. Q. N. Gunaratne, T. Gunnlaugsson, A. J. M. Huxley, C. P. McCoy, J. T. Rademacher and T. E. Rice, *Chem. Rev*., 1997, **97**, 1515–1566.

28. B. K.-L. Wong, G. L. Law, Y.-Y. Yang and W.-T. Wong, *Advanced Materials*, 2006 **18**, 1051-1054.

GRAPHICAL ABSTRACT

A reversible fluorescent-colorimetric chemosensor based on a novel Schiff base for visual detection of CO_3^{2-} in aqueous solution

Anupam Ghorai, Jahangir Mondal, Rukmani Chandra and Goutam K Patra*

Department of Chemistry, Guru Ghasidas Vishwavidyalaya, Bilaspur (C.G)

A novel Schiff base receptor has been fabricated for fluorescent-colorimetric detection of CO_3^{2-} in aqueous medium. Receptor **L** features an excellent selectivity and sensitivity, rapid response, reversibility in sensing CO_3^{2-}. The sensitivity of chemosensor **L** for CO_3^{2-} (96 nM) is the lowest ever found in literature. The chemosensor L has been successfully exploited in real sample analysis for detection of CO_3^{2-}. The geometry of **L** has been optimized both by DFT calculation and single crystal X-ray studies.